Research Paper

Melatonin reverses nasopharyngeal carcinoma cisplatin chemoresistance by inhibiting the Wnt/β-catenin signaling pathway

Jian Zhang[1,*], Tao Xie[1,*], Xi Zhong[2,*], Hua-Li Jiang[3,*], Rong Li[1], Bai-Yao Wang[1], Xiao-Ting Huang[1], Bo-Hong Cen[1], Ya-Wei Yuan[1]

[1]Department of Radiation Oncology, Affiliated Cancer Hospital and Institute of Guangzhou Medical University, State Key Laboratory of Respiratory Diseases, Guangzhou Institute of Respiratory Disease, Affiliated Cancer Hospital and Institute of Guangzhou Medical University, Guangzhou, P. R. China
[2]Department of Radiology, Affiliated Cancer Hospital and Institute of Guangzhou Medical University, Guangzhou, P. R. China
[3]Department of Cardiovascularology, Tungwah Hospital of Sun Yat-Sen University, Dongguan, P.R. China
*Equal contribution

Correspondence to: Ya-Wei Yuan; **email:** yuanyawei@gzhmu.edu.cn
Keywords: chemoresistance, cisplatin, melatonin, nasopharyngeal carcinoma, Wnt/β-catenin
Received: December 1, 2019 **Accepted:** March 16, 2020 **Published:** March 23, 2020

ABSTRACT

Cisplatin (DDP)-based concurrent chemo-radiotherapy is a standard approach to treat locoregionally advanced nasopharyngeal carcinoma (NPC). However, many patients eventually develop recurrence and/or distant metastasis due to chemoresistance. In this study, we aimed to elucidate the effects of melatonin on DDP chemoresistance in NPC cell lines in *vitro* and *vivo*, and we explored potential chemoresistance mechanisms. We found that DDP chemoresistance in NPC cells is mediated through the Wnt/β-catenin signaling pathway. Melatonin not only reversed DDP chemoresistance, but also enhanced DDP antitumor activity by suppressing the nuclear translocation of β-catenin, and reducing expression of Wnt/β-catenin response genes in NPC cells. In *vivo*, combined treatment with DDP and melatonin reduced tumor burden to a greater extent than single drug-treatments in an orthotopic xenograft mouse model. Our findings provide novel evidence that melatonin inhibits the Wnt/β-catenin pathway in NPC, and suggest that melatonin could be applied in combination with DDP to treat NPC.

INTRODUCTION

Nasopharyngeal carcinoma (NPC) is a highly invasive and metastatic head and neck cancer that is prevalent in Southeast Asia, especially southern China. Due to the lack of early symptoms and the aggressiveness of NPC [1], more than 70% of NPC patients present with locoregionally advanced stage at the initial visit, and often have poor disease prognosis [2, 3]. It is essential to elucidate the molecular mechanisms that regulate NPC progression in order to develop novel treatment strategies.

Cisplatin (DDP) is a DNA damaging chemotherapeutic agent, and exerts cytotoxicity and/or induction of apoptosis by forming DNA adducts or by targeting therapeutically relevant cancer signaling pathways [4–6]. DDP is a highly effective treatment for various cancers, including NPC. Platinum-based concurrent chemo-radiotherapy is the standard of care for patients with locoregionally advanced nasopharyngeal carcinoma (LA-NPC) [7, 8]. However, some patients with NPC do not benefit from treatment, and suffer adverse side effects of the additional chemotherapy [9–11], and many patients acquire DDP resistance during chemotherapy for NPC.

Melatonin is a pleiotropically-acting molecule that possesses anti-inflammatory, anti-proliferative, and antioxidant activities in *vitro* and *vivo* [12–16]. Melatonin shows potential as a therapeutic agent, because it not only has synergistic effects with chemotherapeutic drugs, but it can also reduce the side effects of anticancer drugs by neutralizing singlet oxygen species, superoxide anion radicals, peroxyl radicals, and hydrogen peroxide [17–20]. However, the precise therapeutic roles and underlying mechanisms of melatonin activity in NPC are unclear, and it is unknown whether melatonin could attenuate DDP resistance.

In the present study, we explored aberrant signaling pathways mediating DDP chemoresistance in NPC cells, we evaluated whether melatonin may possess anticancer activity on NPC cells, and we investigated whether combinatorial treatment of DDP and melatonin is effective in an orthotopic xenograft mouse model of NPC. We found that melatonin inhibited tumorigenesis of NPC cells and reversed DDP resistance both in *vitro* and *vivo* by inhibiting the Wnt/β-catenin signaling pathway. These results suggest that melatonin may be a useful agent to overcome chemoresistance in the treatment of NPC.

RESULTS

Activation of the Wnt/β-catenin pathway mediates DDP chemoresistance in NPC

To know genomic changes in DDP-resistant cells, we established the DDP-resistant cells, 5-8F and CNE2 cell lines were exposed to increasing concentrations of DDP for more than 6 months. Compared with their parental cells, chemoresistance to DDP was observed in 5-8F/DDP and CNE2/DDP cells. As shown in Supplementary Figure 1, 2.5 μg/mL DDP led to almost 50% cell growth inhibition in both 5-8F and CNE2 cells, respectively. Thus, the resistant NPC cells were continuously maintained in RPMI 1600 medium containing 2.5 μg/mL DDP. DDP-resistant were collected to perform a standard RNA sequencing analysis. RNA sequencing analysis identified 3230 mRNAs differentially expressed in DDP-resistant cells compared to DDP-sensitive cells; 1,757 genes were upregulated and 1,473 genes were downregulated (GSE135083) (Figure 1A).

To identify signaling pathways involved in mediating DDP chemoresistance, we performed bioinformatic pathway analysis of differentially expressed genes between DDP-resistant and DDP-sensitive NPC cells. GO interaction analysis identified Wnt signaling related genes, including DKK1, Wnt7B, Wnt10A, FZD1, FZD2, FZD4, FZD7, FZD8 which likely play important roles in regulating sensitivity to DDP chemotherapy (Supplementary Figure 2). To further explore the mechanisms underlying DDP chemoresistance in NPC, we evaluated molecular pathways associated with DDP chemoresistance. GSEA identified gene sets related to activation of the Wnt/β-catenin signaling pathway, including β-catenin binding (GO: 0008013), Wnt signal pathway (GO: 0060070), Wnt protein binding (GO: 0017147) and Wnt activated activity (GO: 0042813) (Figure 1B; $P < 0.05$). These results indicate that DDP chemoresistance in NPC cells is associated with the Wnt/β-catenin signaling pathway.

Western blot analysis validated differential activation of the Wnt/β-catenin signaling pathway in DDP-resistant cells, and showed an increase in nuclear β-catenin in CNE2 DDP chemoresistant cells (CNE2/DDP) and 5-8F DDP chemoresistant cells (5-8F/DDP) (Figure 1C). Similarly, genes downstream of the Wnt/β-catenin signaling pathway were significantly upregulated in CNE2/DDP and 5-8F/DDP cells, including AXIN2, SOX9, CD44, and CCND2 (Figure 1D, 1E). These data illustrate that the activation of Wnt/β-catenin mediates cisplatin chemoresistance in NPC.

Melatonin suppresses the nuclear translocation of β-catenin in DDP chemoresistant cells

To determine whether melatonin reversed the DDP chemoresistance, CNE2/DDP and 5-8F/DDP cells were treated with 2 mM melatonin for 48 hr. Western blot analysis showed that melatonin decreased the expression of nuclear β-catenin (Figure 2A, 2B). β-catenin functions as a key nuclear effector that controls canonical Wnt signaling in tumorigenesis and metastasis [21–23]. Upon activation of the Wnt pathway, β-catenin translocates into the nucleus and forms β-catenin/TCF complexes, leading to activation of Wnt-mediated gene expression. As shown in Figure 2A and 2B, the downstream genes, c-Myc and CyclinD1, were significantly downregulated in DDP-resistant cells after melatonin treatment. To further verify these findings, we performed qPCR to evaluate the mRNA expression of Wnt pathway genes. Melatonin treatment resulted in downregulation of AXIN2, SOX9, CD44, and CCND2 (Figure 2C), indicating that melatonin may reverse DDP chemoresistance by inhibiting the Wnt/β-catenin pathway.

Immunofluorescence staining showed that DDP-induced accumulation of nuclear β-catenin was decreased in CNE2/DDP and 5-8F/DDP cells following treatment with 2 mM melatonin (Figure 2D, 2E). Moreover, To determine the effects of the melatonin and DDP on the Wnt signaling pathway, the ratio of the activity of a β-catenin-responsive promoter containing TCF binding sites (TOP-flash) to the

activity of a promoter containing mutated TCF binding sites (FOP-flash) was determined in the presence of melatonin or DDP. The expression of β-catenin increased the ratio of TOP-flash activity to FOP-flash activity was considered 100% activity in control group. DDP significantly increased β-catenin activation of TCF-mediated transcription. Melatonin not only decreased β-catenin activation of the TCF promoter, but also reversed the DDP mediated the activation of β-catenin (Figure 2F). Altogether, these data suggest that melatonin reverses the DDP chemoresistance by inhibiting the nuclear translocation of β-catenin.

Melatonin enhances apoptosis and suppresses metastatic behavior in NPC cells

Melatonin effectively induced cell death and suppressed cell growth in 5-8F, CNE2 and SUNE1 cells in a dose-dependent manner (Figure 3A, 3B), while the NP69 nasopharyngeal epithelial cell line was less sensitive to melatonin. Transwell assays demonstrated that treatment with 2 mM melatonin suppressed migration and invasion of 5-8F and CNE2 cells (Figure 3C, 3D). These results show melatonin can inhibit malignant characteristics of NPC cells.

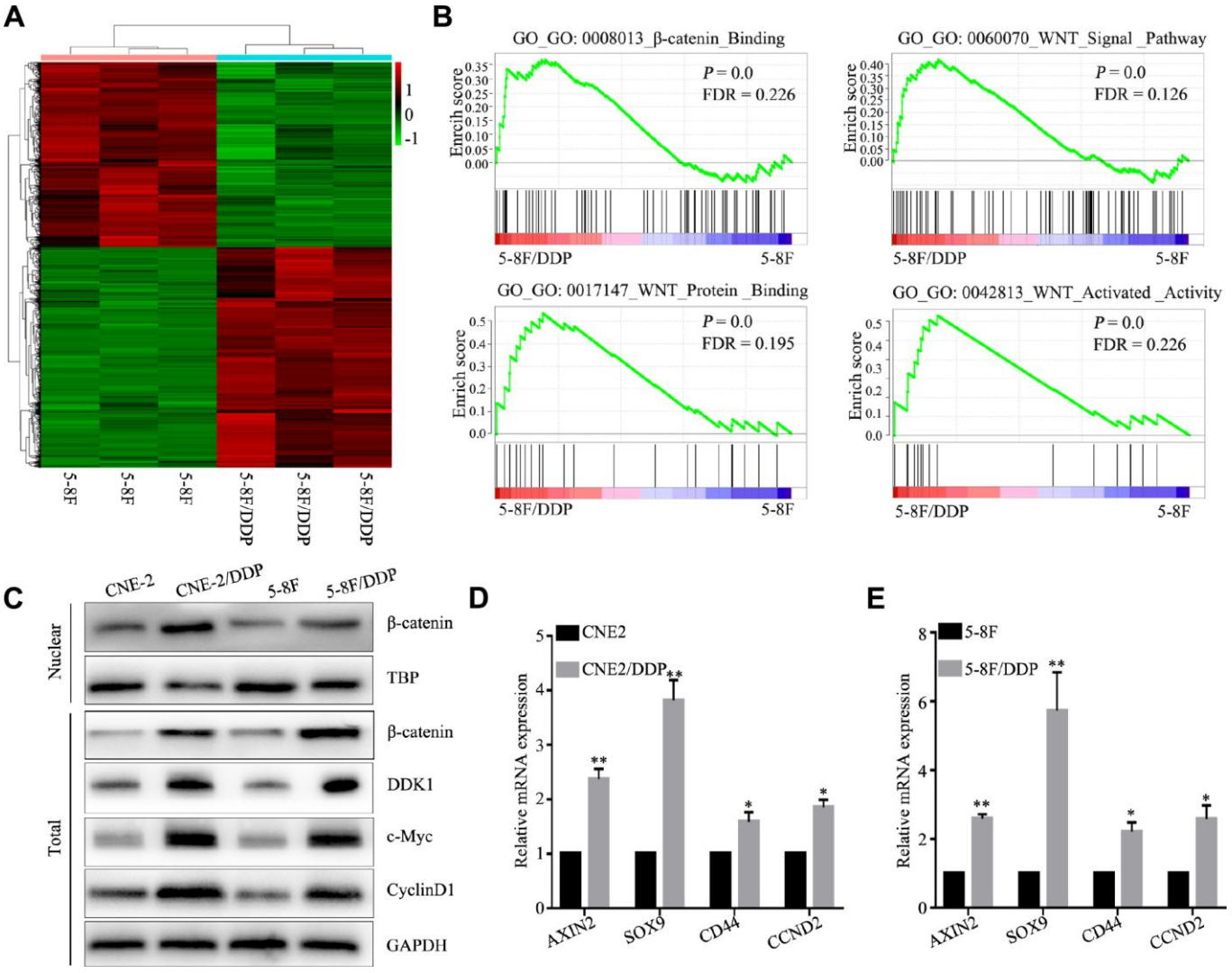

Figure 1. DDP chemoresistance in NPC cells is mediated through activation of the Wnt/β-catenin pathway. (**A**) Heatmap of differentially expressed genes in 5-8F and 5-8F/DDP cell lines by RNA sequencing. (**B**) Differentially enriched Wnt/β-catenin pathway-related signatures between 5-8F and 5-8F/DDP cell lines, determined by gene set enrichment analysis (GSEA). (**C**) Protein expression of Wnt/β-catenin in the CNE2 and CNE2/DDP, 5-8F and 5-8F/DDP cell lines, as determined by western blot. (**D**, **E**) mRNA expression of the Wnt/β-catenin downstream genes (AXIN2, SOX9, CD44 and CCND2) in CNE2 and CNE2/DDP cell lines (**D**) and 5-8F and 5-8F/DDP cell lines (**E**) as determined by qPCR. All of the experiments were performed at least three times. Data presented are the mean ± SD; $^{**}P < 0.01$ compared with using the Student *t*-test.

Melatonin reverses DDP chemoresistance in NPC DDP-resistant cells

To further know the function of melatonin on DDP-resistant cells, CNE2/DDP and 5-8F/DDP cells were further treated with 2 mM melatonin. As shown in Figure 4A and 4B, Melatonin significantly inhibited cell growth in CNE2/DDP and 5-8F/DDP cells after treated with melatonin 48h, 72h and 96h. Transwell assays showed that the migration and invasion abilities were

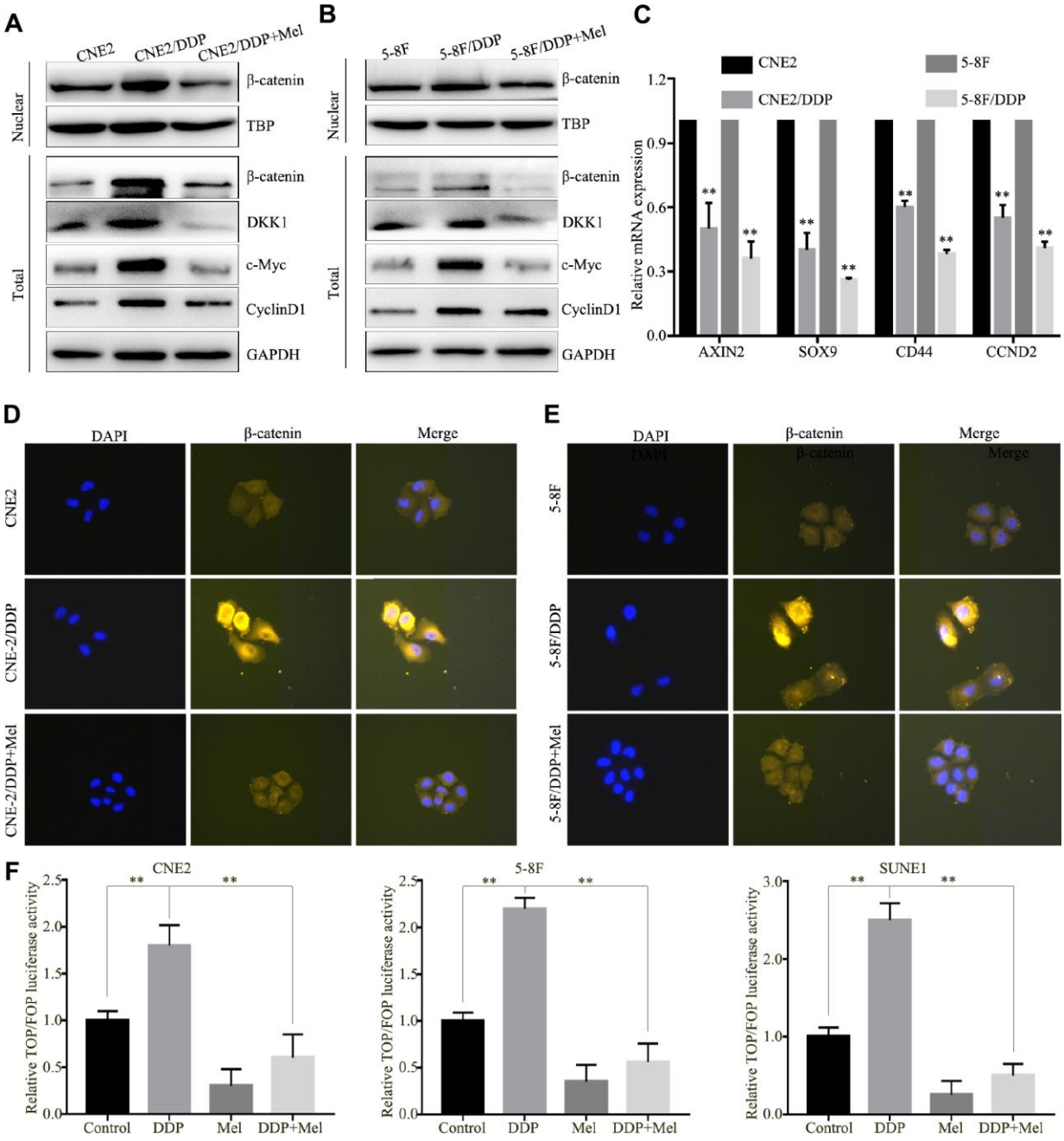

Figure 2. Melatonin reverses DDP chemoresistance by inhibiting β-catenin nuclear translocation. (**A**, **B**) Protein expression of β-catenin, DKK1, c-Myc and CylincD1 in the CNE2 and CNE2/DDP (**A**), 5-8F and 5-8F/DDP cell lines (**B**) treated with melatonin (2 mM) for 48 hr, as determined by western blot. (**C**) mRNA expression of Wnt/β-catenin downstream genes (AXIN2, SOX9, CD44 and CCND2) in CNE2 and CNE2/DDP, 5-8F and 5-8F/DDP cell lines treated with melatonin (2 mM) for 48 hr, as determined by qPCR. (**D**, **E**) Representative images of immunofluorescent staining for β-catenin in CNE2 and CNE2/DDP (**D**), 5-8F and 5-8F/DDP (**E**) treated with or without melatonin (2 mM) for 48 hr. (**F**) Relative luciferase activity of NPC cells transfected with the TOP/FOPFlash vector and pRL-TK vector. Data presented are the mean ± SD; $^{**}P < 0.01$ compared with control using Student *t*-test.

significantly decreased after melatonin treatment (Figure 4C, 4D). Colony formation assay further indicated that melatonin could significantly reduce the colony growth in CNE2/DDP and 5-8F/DDP cells (Figure 4E). These results indicate that melatonin can reverses DDP chemoresistance in NPC cells.

Melatonin and DDP combination inhibits NPC cell growth

The effects of melatonin treatment on cell growth and DDP sensitivity were evaluated in four NPC cell lines: CNE2, 5-8F, HONE1, and SUNE1. After four days of culture with 1 μg/ml DDP, the growth of all NPC cell lines was significantly suppressed. Additionally, the growth was further suppressed after addition of 1 mM melatonin treatment (Figure 5A–5D), suggesting that melatonin and DDP may synergize to suppress growth of NPC cells. Treatment with either melatonin or DDP alone delayed colony growth in CNE2, 5-8F, HONE1, and SUNE1 cells, and treatment with a combination of DDP and melatonin showed synergistic suppression of colony formation (Figure 5E, 5F). These results

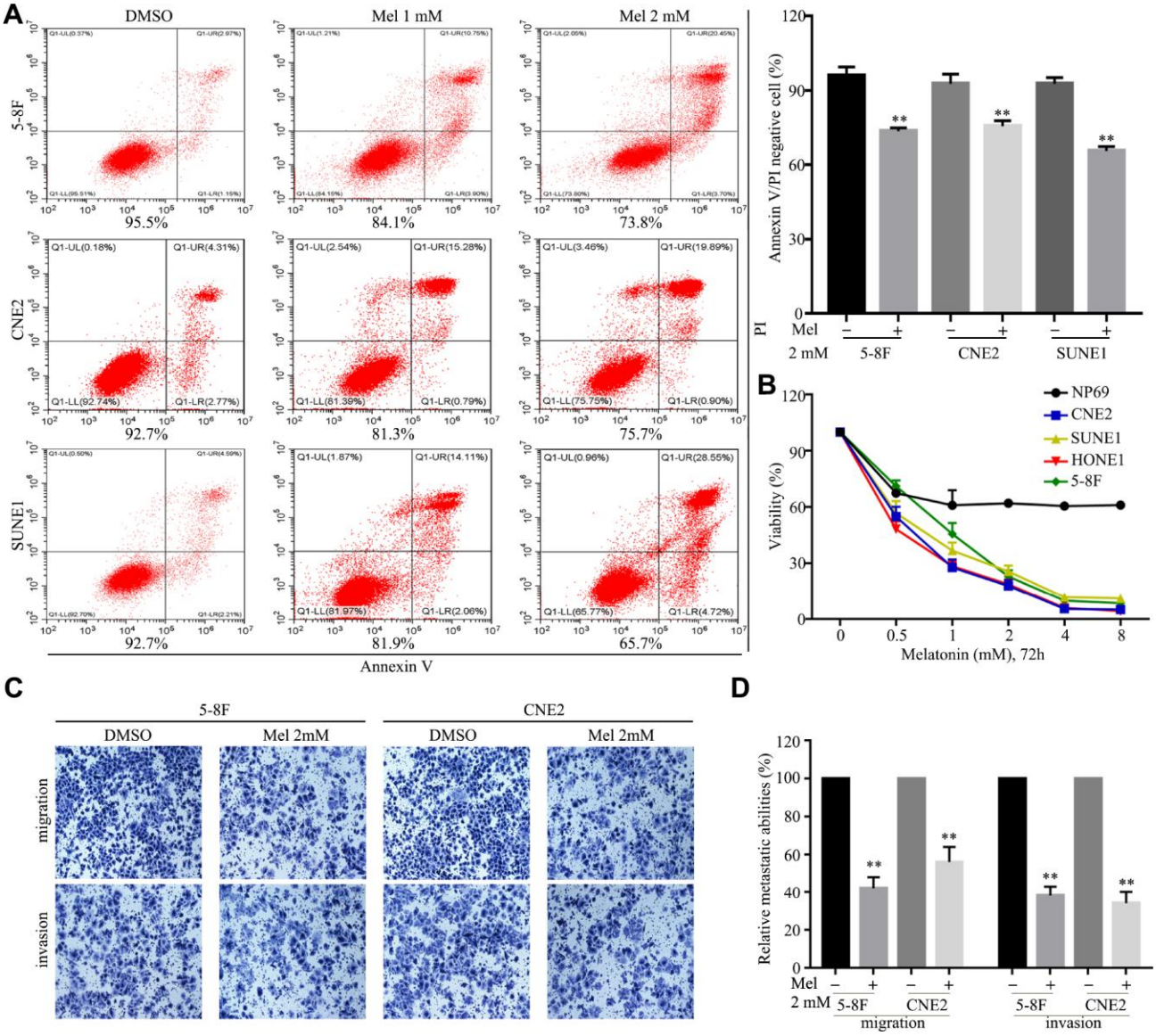

Figure 3. Melatonin inhibits malignant properties of NPC cells. (**A**) Representative images (left panel) and quantification (right upper panel) of cell apoptosis in the indicated cells treated with melatonin (Mel, 48 hr), as determined by AnnexinV/propidium iodide (PI) assay. (**B**) The cell viability of the indicated cells incubated with melatonin (72 hr) was determined by CCK-8 assay. (**C**, **D**) Images and quantification of migrated (**C**) and invaded (**D**) NPC cells treated with melatonin (2 mM) for 24 hr were analyzed in transwell assays. Data presented are the mean ± SD; $^{**}P < 0.01$ compared with control using Student *t*-test.

suggest that melatonin enhances the inhibition of cell proliferation induced by DDP in NPC cell lines.

Melatonin and DDP combination inhibits NPC tumor metastasis *in vivo*

To further determine if treatment with a combination of DDP and melatonin may be a potential therapeutic strategy to treat NPC, we examined the antitumor capability of melatonin in a xenograft nude mouse model. HONE1 cells were injected into the tail veins of nude mice, and mice were randomly assigned to four treatment groups (n = 3 per group). Treatment with DDP, melatonin, both agents, and vehicle control began2 weeks after injection, and lasted for 4 weeks (Figure 6A). While DDP or melatonin treatment alone showed some

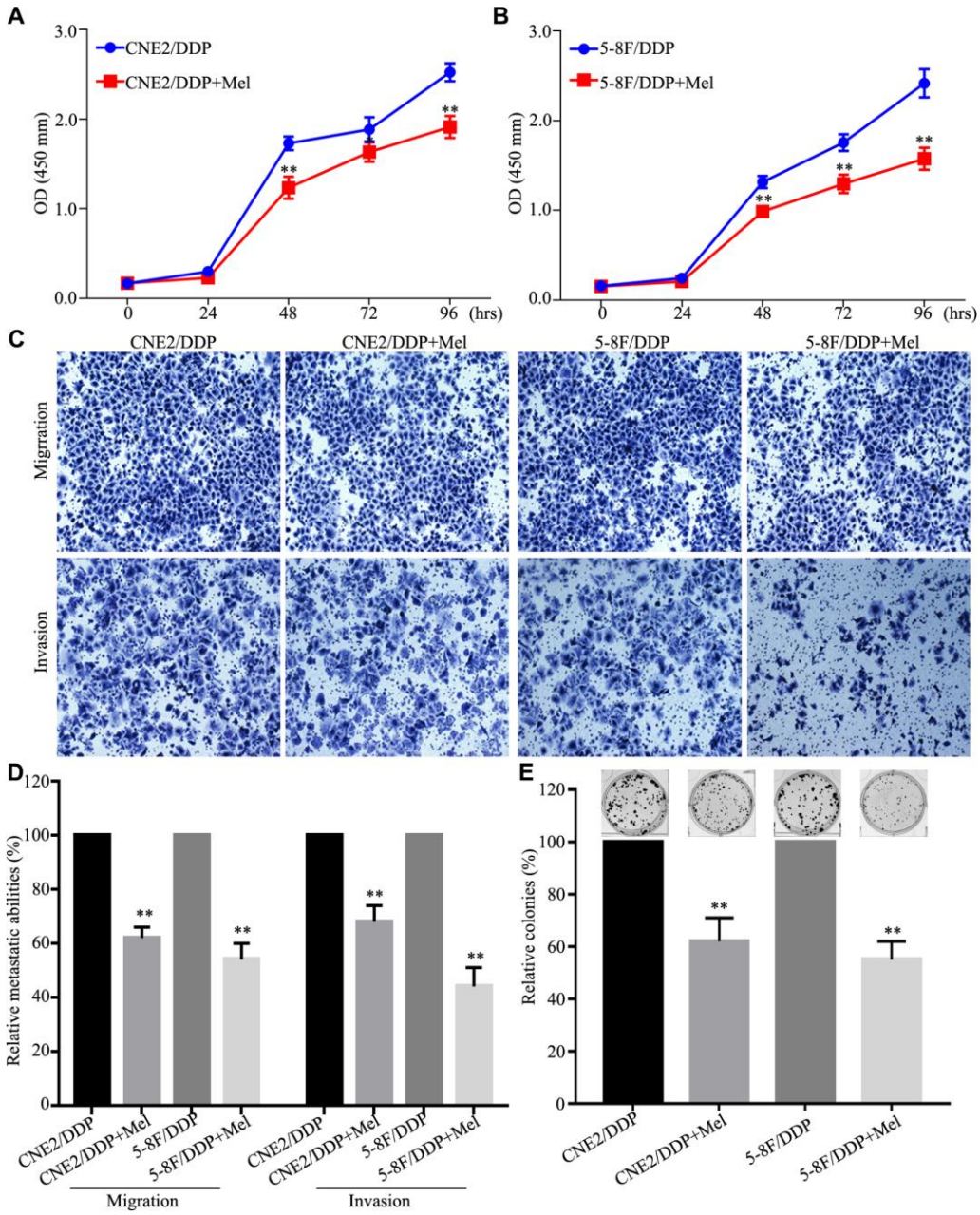

Figure 4. Melatonin reverses DDP chemoresistance in NPC DDP-resistant cells. (**A**, **B**) The cell viability of the CNE2/DDP (**A**) and 5-8F/DDP (**B**) cells treated with melatonin (2 mM) was determined by CCK-8 assay. (**C**, **D**) Images (**C**) and quantification (**D**) of transwell migration and invasion assays. (**E**) Images (up) and quantification (down) clonogenic colony formation assays of the CNE2/DDP and 5-8F/DDP cells treated with melatonin for 2 weeks. All of the experiments were performed at least three times. Data presented are the mean ± SD; $^{**}P < 0.01$, $^{*}P < 0.05$ compared with control using Student *t*-test.

suppressive effects compared to the control group at 4 weeks (Figure 6B), combination treatment with DDP and melatonin showed a significant reduction in tumor burden (Figure 6C–6E). HE and IHC staining also showed that the combination of DDP and melatonin resulted in reduction in tumor volume, lower cell proliferation indices (Ki67-positive), and lower expression of β-catenin (β-catenin-positive) compared with DDP or melatonin alone treatments (Figure 6F). Collectively these results indicate that treatment with a combination of DDP and melatonin inhibits metastasis of NPC cells *in vivo*.

DISCUSSION

NPC is one of the most common head and neck cancers in Southern China and Southeast Asia [24]. Most NPC cells are poorly differentiated squamous cells and are highly sensitive to chemotherapy, and chemotherapy remains the mainstay of treatment for NPC.

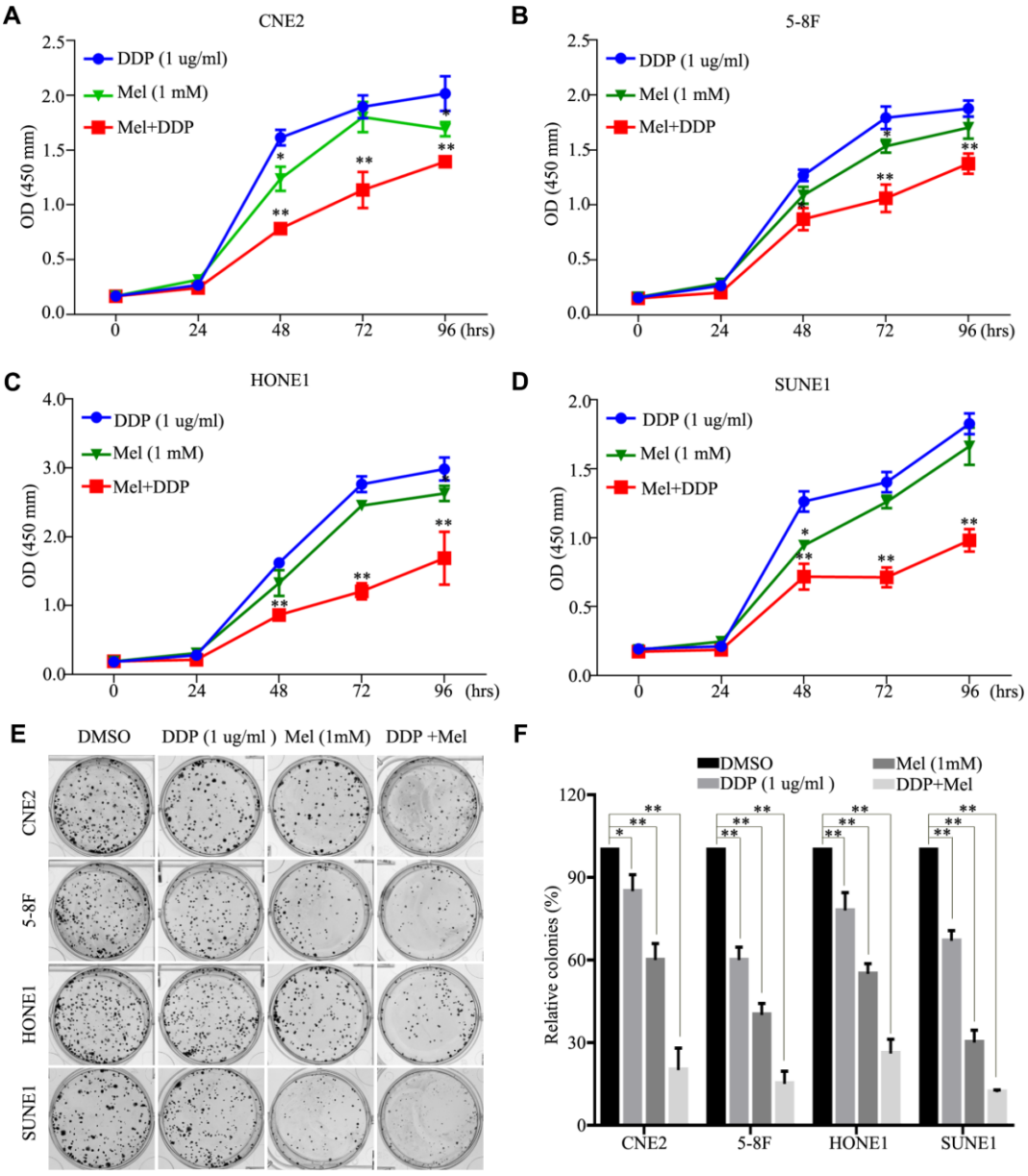

Figure 5. Effects of melatonin and DDP combination on malignant properties of nasopharyngeal carcinoma (NPC) cells. (**A**–**D**) The cell viability of the CNE2 (**A**), 5-8F (**B**), HONE1 (**C**) and SUNE1 (**D**) cells incubated with melatonin (72 hr) (green line) alone and DDP alone (blue line) or melatonin with DDP combination (red line) was determined by CCK-8 assay. (**E**, **F**) Images (**E**) and quantification (**F**) clonogenic colony formation assays of the indicated cells treated with melatonin for 2 weeks. All of the experiments were performed at least three times. Data presented are the mean ± SD; $^{**}P < 0.01$, $^{*}P < 0.05$ compared with control using Student *t*-test.

In this study, we report that melatonin inhibited activation of the Wnt/β-catenin pathway by suppressing β-catenin nuclear translocation, reversing DDP chemoresistance of NPC cells *in vitro* and *in vivo* (Figure 7), and indicating that treatment with a combination of melatonin and DDP may be a constructive therapeutic strategy to treat NPC.

The chemotherapeutic drug DDP is a standard initial treatment for patients with LA-NPC [25–27]. Phase 2 trials have shown that gemcitabine plus cisplatin is an effective chemotherapeutic strategy in patients with NPC [28–30]. We performed a phase 3 trial which confirmed that the combination of docetaxel, cisplatin, and fluorouracil (TPF) chemotherapy to CCRT can

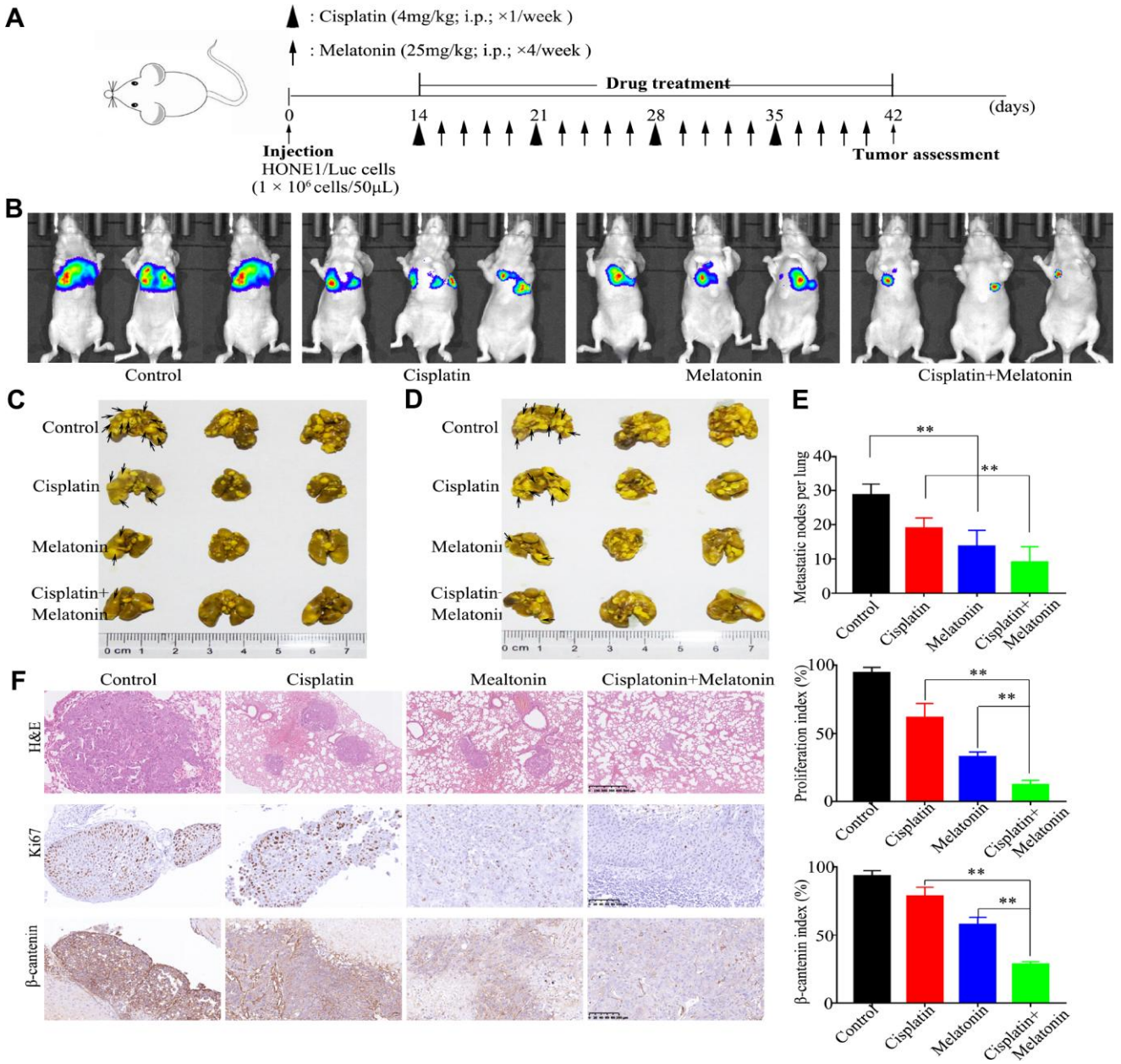

Figure 6. Antitumor activity of melatonin plus DDP *in vivo* in a lung metastasis model. (**A**) Tumor progression timeline with experimental treatment time points. (**B**) Tumor cell luminescence from each mouse in each group was acquired on treatment day 28. (**C**, **D**) Representative front images (**C**) and back images (**D**) of macroscopic lung metastases, arrowheads indicate the metastatic nodes. (**E**) Quantification of the average number of macroscopic metastatic nodes formed on the lung surface. (**F**) Paraffin-embedded tumor sections were stained with H&E, anti-Ki67, and β-catenin antibodies (Scar bar: 100 μm). Right panel: quantification of the proliferation index and β-catenin index in tumor sections. These animal experiments were repeated once (n = 3 mice per treatment group). Data presented are the mean ± SD; ***P* < 0.01 compared with control using Student *t*-test.

significantly improve 3-year distant metastasis-free survival (DMFS) for LA-NPC patients [30]. However, this treatment strategy only results in a 7% improvement in control of disease metastatic. The limited effect is attributable to many factors, including extrinsic or intrinsic resistance to conventional chemotherapy.

DDP has been reported to activate the Wnt/β-catenin through some ligand-independent regulatory mechanisms, which can reduce its antitumor activity [31]. Moreover, antagonism of β-catenin reverses cisplatin resistance in DDP-treated mouse models [32]. In the current study, we showed that DDP resistance resulted in an increase in nuclear β-catenin and in the expression levels of β-catenin in NPC cells. Wnt/β-catenin activation is involved in the induction of stemness, inhibition of differentiation, and regulation of gene products that promote proliferation, migration, and invasion of NPC cells, which contributes to chemoresistance in NPC [33–35]. Therefore, the Wnt/β-catenin pathway is a potential target for developing novel therapeutic strategies for NPC.

Melatonin mitigates tumorigenesis, progression, and metastasis of many types of cancer, including breast cancer, ovarian cancer, colorectal cancer, and lung cancer [36–39]. Melatonin inhibits 12-O-tetradecanoylphorbol-3-acetate-induced cell motility by regulating expression of matrix metalloproteinase-9 (MMP-9) in NPC cells [40]. In the present study, we investigated the responses of NPC cells to treatment with a combination of melatonin and DDP. Both DDP and melatonin have been shown to individually inhibit cancer cell growth in many studies, but they have never been combined together to treat nasopharyngeal cancer. Our results showed that DDP chemoresistance in NPC cells is mediated through activation of the Wnt/β-catenin signaling pathway. We show that melatonin can reverse DDP chemoresistance in NPC cell lines and can enhance the inhibitory effects of DDP by decreasing phosphorylation of β-catenin. However, underlying mechanism for this requires further elucidation in future studies.

In conclusion, we report that chemoresistance to DDP in NPC is mediated through activation of the Wnt/β-catenin pathway, and that melatonin treatment can reverse DDP chemoresistance and enhance the antitumor effects of DDP in NPC. Therefore, combination treatment with melatonin and DDP may be a promising clinical approach to treat patients with NPC.

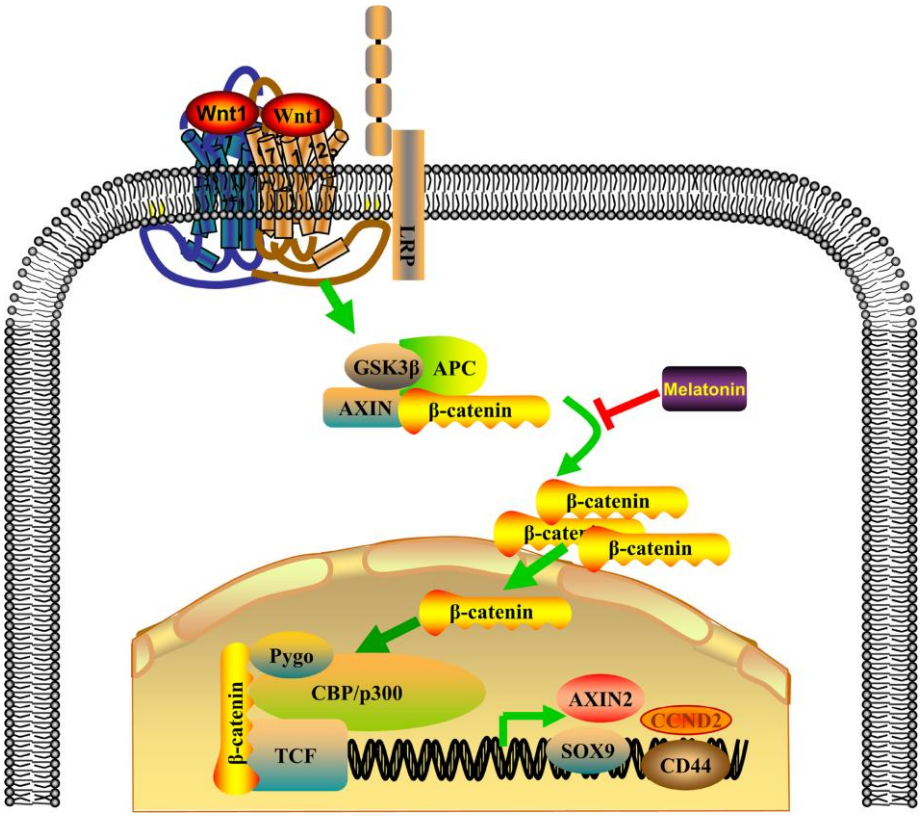

Figure 7. Proposed model of the combinatorial effect of DDP and melatonin on NPC cells.

MATERIALS AND METHODS

Cell lines and cell culture

Human NPC cell lines (CNE2, SUNE1, HONE1, and 5-8F) were cultured in RPMI-1640 (Invitrogen, USA) supplemented with 5% FBS (Gibco). Cisplatin resistant cell lines, 5-8F/DDP and CNE2/DDP, were established by long-term culture in increasing concentrations of DDP, up to 2.5 μg/ml, for more than 6 months. The normal human nasopharyngeal epithelial cell line, NP69, was grown in KSF medium (Invitrogen) supplemented with bovine pituitary extract (BD Biosciences, San Jose, CA). All nasopharyngeal epithelial cell lines and NPC cell lines were generously provided by Professor Musheng Zeng (Sun Yat-sen University Cancer Center, China).

Reagents

Cisplatin (DDP) was purchased from Selleck Chemicals (Houston, TX, USA) and dissolved in water. Melatonin was purchased from Sigma-Aldrich (St.Louis, MO, USA) and dissolved in DMSO.

Whole transcriptome expression analysis (RNA-seq)

Total RNA was extracted from 5-8F and 5-8F/DDP cells. After removal of the RNA-later reagent, samples were stored at –80°C. RNA quality was assessed using an Agilent Bioanalyzer (Agilent Technologies, Santa Clara, CA, USA), and high-quality RNA samples (RNA integrity numbers >7.0) were used for RNA-seq analysis.

Total RNA (1 μg) was used to generate sequencing libraries using the TruSeq Stranded mRNA Sample Prep Kit (lllumina, San Diego, CA, USA) following the manufacturer's instructions. Libraries were subjected to paired-end sequencing of 43-bp reads using a NextSeq500 System (Illumina) with a NextSeq500 High Output Kit (Illumina). The reads were aligned to the UCSC reference human genome 19 (hg19) using Spliced Transcripts Alignment to a Reference (STAR) software v2.3.1 (DNASTAR, Inc. Madison, WI, USA). Differentially expressed genes (DEGs) were detected using DESeq v1.24.0. Genes with significant expression differences in 5-8F/DDP compared with 5-8F cells were determined ($|\log_2(\text{fold change})| > 1.5$, adjusted $P < 0.05$).

Gene set enrichment analysis (GSEA)

A GSEA software tool (version 2.0.13, https://www.broadinstitute.org/gsea/) was used to identify KEGG pathways (MSigDB, version 4.0) that are overrepresented in the genes that were upregulated or downregulated between the 5-8F and 5-8F/DDP cells. Briefly, an enrichment score was calculated for each gene set (i.e., KEGG pathway) by ranking gene expression difference.

Western blot

Total protein was extracted from cells using RIPA lysis buffer (P0013B, Beyotime, China) or Nuclear and Cytoplasmic Protein Extraction Kit (P0027, Beyotime, China). Protein concentrations were quantified using a BCA Protein Assay Kit. Proteins were separated using SDS-PAGE, then electrophoretically transferred to membranes. Membranes were blocked with 5% non-fat milk and incubated overnight at 4°C with primary antibodies (Supplementary Table 1).

RNA isolation and quantitative PCR

Total RNA was extracted using TRIzol regent (Life Technology, Carlsbad, USA) and converted to cDNA using a M-MLV reverse transcriptase kit (Promega). Quantitative PCR was performed and analyzed as described previously [41]. The primer sequences are shown in Supplementary Table 2.

Immunofluorescence

Cells were fixed with methyl alcohol, permeabilized with 0.5% Triton X-100, and incubated with primary antibodies. Cells were subsequently incubated with species-matched secondary antibodies (Supplementary Table 2). Nuclei were stained with DAPI (Sigma) and fluorescence images were obtained using a confocal scanning microscope (Olympus FV1000).

TOP/FOPFlash reporter assay

TOP/FOPFlash reporter assays were used to determine the transcriptional activity of the Wnt/β-catenin pathway. The reporter plasmids containing TOPFlash and mutated FOPFlash TCF/LEF DNA binding sites were purchased from Addgene. Briefly, NPC cells and DDP resistant cells were seeded in 96-well plates and transfected with the TOP/FOPFlash vector and pRL-TK vector (Promega). Luciferase activity was measured using the Promega Dual-Luciferase Reporter Assay System 24 h after transfection. The firefly luciferase activity in each sample was normalized to the *Renilla* luciferase activity within that sample.

Cell viability assay

Cells (1×10^3) were seeded into 96-well plates and incubated for the indicated time periods (1, 2, 3, 4, 5 days). On the indicated days, CCK-8 reagent (10 μl; Dojindo, Tokyo, Japan) was added to each well and

incubated for 2 h. After incubation, the absorbance at 450 nm in each well was read using a spectrophotometer.

Colony formation assay

Cells (0.3×10^3) were seeded into 6-well plates and cultured for 1 week (CNE2 and HONE1 cells) or 2 weeks (5-8F and SUNE1 cells). Colonies that formed were fixed with methyl alcohol, stained with crystal violet, and quantified.

Cell apoptosis

Cells were lifted from culture plastic, centrifuged, and resuspended in a PBS buffer to form a single-cell suspension. Cell death in NPC cell lines induced by melatonin was analyzed by flow cytometry using Annexin-V/propidiumiodide (PI), assays according to the manufacturer's instructions (BD Biosciences, Bedford, USA).

Transwell migration and invasion assays

The effects of DDP and/or melatonin on the migratory and invasive ability of NPC cell lines were evaluated by transwell assays. Cells (5×10^4 or 1×10^5) were suspended in 200 μL of serum-free medium and plated into transwell chambers with 8 μm pores (Corning) that were uncoated (migration assay) or coated with Matrigel (BD Biosciences) (invasion assay). Cells were cultured at 37°C for 12 hours or 24 hours. Methanol was used to fix the cells that had migrated or invaded into the lower chamber. Cells were stained with 1% crystal violet solution and manually counted.

Tumor xenografts experiments in vivo

BALB/c nude mice (six-week old) were obtained from Charles River Laboratories (Beijing, China). HONE1-luciferase cells (1×10^6) were resuspended in 200 μL serum-free medium and injected intravenously into the tail veins. After 6 weeks, the mice were randomly assigned (n = 3 per group) to receive the following treatments on a weekly schedule: Group 1 served as a control and received no treatment; group 2 received 4 mg/kg intraperitoneal DDP once a week; group 3 was treated with 25 mg/kg intraperitoneal melatonin on four consecutive days per week; group 4 was treated with 4 mg/kg, intraperitoneal DDP once a week followed by 25 mg/kg melatonin each day for four days. Treatments were continued for 4 weeks.

After euthanasia, lung tissues were fixed to determine the numbers of metastatic nodes formed on the surface of lungs. The tissues were paraffin-embedded, and serial 5-μm tissue sections were cut and stained with hematoxylin–eosin (HE) to examine metastatic nodes in the lungs as previously described [42, 43]. All animal research was conducted in accordance with the regulations approved by the Animal Care and Use Ethnic Committee of Affiliated Cancer Hospital and Institute of Guangzhou Medical University, and all efforts were made to minimize animal suffering.

Immunohistochemistry (IHC) assay

Tissue sections were deparaffinized with xylene and rehydrated with a gradient of ethanol to distilled water. After treatment with citrate buffer (pH 6.0), the tissue sections were pre-incubated with hydrogen peroxide and blocked with goat serum (Beyotime). The sections were then incubated with primary antibodies (Supplementary Table 2) at 4°C overnight. Sections were then incubated with secondary antibody working solution (Dako, GK500705) for 1 h at 37°C. Finally, a the sections were stained with a DAB Substrate Kit (Invitrogen, USA) for 5 min to observe protein expression, as previously described [44].

Statistical analysis

All statistical analyses were carried out using SPSS 16.0 statistical software (SPSS Inc.). All data presented as the mean ± SD were derived from no less than three independent experiments. Differences between groups were analyzed using the Student's t test or the $\chi 2$ test. All tests were two-tailed; $P < 0.05$ was considered statistically significant.

Abbreviations

NPC: Nasopharyngeal carcinoma; DDP: Cisplatin; LA-NPC: locoregionally advanced nasopharyngeal carcinoma; DEGs: Differentially expressed genes; GSEA: Gene set enrichment analysis; IHC: Immunohistochemistry; DMFS: distant metastasis-free survival.

AUTHOR CONTRIBUTIONS

JZ, TX and XZ carried out all the experiments, prepared figures and drafted the manuscript. HJ, RL, BW, XH and BC participated in data analysis and interpretation of results. JZ and YY designed the study, participated in data analysis. All authors read and approved the manuscript.

ACKNOWLEDGMENTS

We would like to thank the native English-speaking scientists of Elixigen Company (Huntington Beach, California) for editing our manuscript.

CONFLICTS OF INTEREST

The authors declare that they have no conflicts of interest.

FUNDING

This work was supported by grants from the Social Science and Technology Development Key Project of Dongguan (201750715046462); Guangzhou Key Medical Discipline Construction Project Fund (B195002004042); Open Funds of State Key Laboratory of Oncology in South China (KY013711).

REFERENCES

1. Chen W, Zheng R, Baade PD, Zhang S, Zeng H, Bray F, Jemal A, Yu XQ, He J. Cancer statistics in China, 2015. CA Cancer J Clin. 2016; 66:115–32. https://doi.org/10.3322/caac.21338 PMID:26808342

2. Chua ML, Wee JT, Hui EP, Chan AT. Nasopharyngeal carcinoma. Lancet. 2016; 387:1012–24. https://doi.org/10.1016/S0140-6736(15)00055-0 PMID:26321262

3. Lai SZ, Li WF, Chen L, Luo W, Chen YY, Liu LZ, Sun Y, Lin AH, Liu MZ, Ma J. How does intensity-modulated radiotherapy versus conventional two-dimensional radiotherapy influence the treatment results in nasopharyngeal carcinoma patients? Int J Radiat Oncol Biol Phys. 2011; 80:661–68. https://doi.org/10.1016/j.ijrobp.2010.03.024 PMID:20643517

4. Amable L. Cisplatin resistance and opportunities for precision medicine. Pharmacol Res. 2016; 106:27–36. https://doi.org/10.1016/j.phrs.2016.01.001 PMID:26804248

5. Chen SH, Kuo CC, Li CF, Cheung CH, Tsou TC, Chiang HC, Yang YN, Chang SL, Lin LC, Pan HY, Chang KY, Chang JY. O(6) -methylguanine DNA methyltransferase repairs platinum-DNA adducts following cisplatin treatment and predicts prognoses of nasopharyngeal carcinoma. Int J Cancer. 2015; 137:1291–305. https://doi.org/10.1002/ijc.29486 PMID:25693518

6. Wang K, Chen Z, Long L, Tao Y, Wu Q, Xiang M, Liang Y, Xie X, Jiang Y, Xiao Z, Yan Y, Qiu S, Yi B. iTRAQ-based quantitative proteomic analysis of differentially expressed proteins in chemoresistant nasopharyngeal carcinoma. Cancer Biol Ther. 2018; 19:809–24. https://doi.org/10.1080/15384047.2018.1472192 PMID:30067426

7. Baujat B, Audry H, Bourhis J, Chan AT, Onat H, Chua DT, Kwong DL, Al-Sarraf M, Chi KH, Hareyama M, Leung SF, Thephamongkhol K, Pignon JP, and MAC-NPC Collaborative Group. Chemotherapy in locally advanced nasopharyngeal carcinoma: an individual patient data meta-analysis of eight randomized trials and 1753 patients. Int J Radiat Oncol Biol Phys. 2006; 64:47–56. https://doi.org/10.1016/j.ijrobp.2005.06.037 PMID:16377415

8. Saurin JC, Gutknecht C, Napoleon B, Chavaillon A, Ecochard R, Scoazec JY, Ponchon T, Chayvialle JA. Surveillance of duodenal adenomas in familial adenomatous polyposis reveals high cumulative risk of advanced disease. J Clin Oncol. 2004; 22:493–98. https://doi.org/10.1200/JCO.2004.06.028 PMID:14752072

9. Liu RY, Dong Z, Liu J, Zhou L, Huang W, Khoo SK, Zhang Z, Petillo D, Teh BT, Qian CN, Zhang JT. Overexpression of asparagine synthetase and matrix metalloproteinase 19 confers cisplatin sensitivity in nasopharyngeal carcinoma cells. Mol Cancer Ther. 2013; 12:2157–66. https://doi.org/10.1158/1535-7163.MCT-12-1190 PMID:23956056

10. Lam WK, Jiang P, Chan KC, Peng W, Shang H, Heung MM, Cheng SH, Zhang H, Tse OY, Raghupathy R, Ma BB, Hui EP, Chan AT, et al. Methylation analysis of plasma DNA informs etiologies of Epstein-Barr virus-associated diseases. Nat Commun. 2019; 10:3256. https://doi.org/10.1038/s41467-019-11226-5 PMID:31332191

11. Proctor RN. FDA's new plan to reduce the nicotine in cigarettes to sub-addictive levels could be a game-changer. Tob Control. 2016; 26:487–88. https://doi.org/10.1136/tobaccocontrol-2017-053978 PMID:28831030

12. Tan DX, Manchester LC, Esteban-Zubero E, Zhou Z, Reiter RJ. Melatonin as a Potent and Inducible Endogenous Antioxidant: synthesis and Metabolism. Molecules. 2015; 20:18886–906. https://doi.org/10.3390/molecules201018886 PMID:26501252

13. Volt H, García JA, Doerrier C, Díaz-Casado ME, Guerra-Librero A, López LC, Escames G, Tresguerres JA, Acuña-Castroviejo D. Same molecule but different expression: aging and sepsis trigger NLRP3 inflammasome activation, a target of melatonin. J Pineal Res. 2016; 60:193–205. https://doi.org/10.1111/jpi.12303 PMID:26681113

14. Sainz RM, Mayo JC, Rodriguez C, Tan DX, Lopez-Burillo S, Reiter RJ. Melatonin and cell death: differential actions on apoptosis in normal and cancer cells. Cell Mol Life Sci. 2003; 60:1407–26. https://doi.org/10.1007/s00018-003-2319-1 PMID:12943228

15. Martín V, García-Santos G, Rodriguez-Blanco J, Casado-Zapico S, Sanchez-Sanchez A, Antolín I, Medina M, Rodriguez C. Melatonin sensitizes human malignant glioma cells against TRAIL-induced cell death. Cancer Lett. 2010; 287:216–23. https://doi.org/10.1016/j.canlet.2009.06.016 PMID:19632770

16. Melchers LJ, Mastik MF, Samaniego Cameron B, van Dijk BA, de Bock GH, van der Laan BF, van der Vegt B, Speel EJ, Roodenburg JL, Witjes MJ, Schuuring E. Detection of HPV-associated oropharyngeal tumours in a 16-year cohort: more than meets the eye. Br J Cancer. 2015; 112:1349–57. https://doi.org/10.1038/bjc.2015.99 PMID:25867270

17. Mills E, Wu P, Seely D, Guyatt G. Melatonin in the treatment of cancer: a systematic review of randomized controlled trials and meta-analysis. J Pineal Res. 2005; 39:360–66. https://doi.org/10.1111/j.1600-079X.2005.00258.x PMID:16207291

18. Jung KH, Hong SW, Zheng HM, Lee HS, Lee H, Lee DH, Lee SY, Hong SS. Melatonin ameliorates cerulein-induced pancreatitis by the modulation of nuclear erythroid 2-related factor 2 and nuclear factor-kappaB in rats. J Pineal Res. 2010; 48:239–50. https://doi.org/10.1111/j.1600-079X.2010.00748.x PMID:20210857

19. Park SY, Jang WJ, Yi EY, Jang JY, Jung Y, Jeong JW, Kim YJ. Melatonin suppresses tumor angiogenesis by inhibiting HIF-1alpha stabilization under hypoxia. J Pineal Res. 2010; 48:178–84. https://doi.org/10.1111/j.1600-079X.2009.00742.x PMID:20449875

20. Shiu SY, Pang B, Tam CW, Yao KM. Signal transduction of receptor-mediated antiproliferative action of melatonin on human prostate epithelial cells involves dual activation of Gα(s) and Gα(q) proteins. J Pineal Res. 2010; 49:301–11. https://doi.org/10.1111/j.1600-079X.2010.00795.x PMID:20695976

21. Clevers H. Wnt/beta-catenin signaling in development and disease. Cell. 2006; 127:469–80. https://doi.org/10.1016/j.cell.2006.10.018 PMID:17081971

22. Valenta T, Hausmann G, Basler K. The many faces and functions of β-catenin. EMBO J. 2012; 31:2714–36. https://doi.org/10.1038/emboj.2012.150 PMID:22617422

23. Li VS, Ng SS, Boersema PJ, Low TY, Karthaus WR, Gerlach JP, Mohammed S, Heck AJ, Maurice MM, Mahmoudi T, Clevers H. Wnt signaling through inhibition of β-catenin degradation in an intact Axin1 complex. Cell. 2012; 149:1245–56. https://doi.org/10.1016/j.cell.2012.05.002 PMID:22682247

24. Cao SM, Simons MJ, Qian CN. The prevalence and prevention of nasopharyngeal carcinoma in China. Chin J Cancer. 2011; 30:114–19. https://doi.org/10.5732/cjc.010.10377 PMID:21272443

25. Noronha V, Joshi A, Patil VM, Agarwal J, Ghosh-Laskar S, Budrukkar A, Murthy V, Gupta T, D'Cruz AK, Banavali S, Pai PS, Chaturvedi P, Chaukar D, et al. Once-a-Week Versus Once-Every-3-Weeks Cisplatin Chemoradiation for Locally Advanced Head and Neck Cancer: A Phase III Randomized Noninferiority Trial. J Clin Oncol. 2018; 36:1064–72. https://doi.org/10.1200/JCO.2017.74.9457 PMID:29220295

26. Xiang M, Colevas AD, Holsinger FC, Le QX, Beadle BM. Survival After Definitive Chemoradiotherapy With Concurrent Cisplatin or Carboplatin for Head and Neck Cancer. J Natl Compr Canc Netw. 2019; 17:1065–73. https://doi.org/10.6004/jnccn.2019.7297 PMID:31487677

27. Szturz P, Cristina V, Herrera Gómez RG, Bourhis J, Simon C, Vermorken JB. Cisplatin Eligibility Issues and Alternative Regimens in Locoregionally Advanced Head and Neck Cancer: Recommendations for Clinical Practice. Front Oncol. 2019; 9:464. https://doi.org/10.3389/fonc.2019.00464 PMID:31245288

28. He X, Ou D, Ying H, Zhu G, Hu C, Liu T. Experience with combination of cisplatin plus gemcitabine chemotherapy and intensity-modulated radiotherapy for locoregionally advanced nasopharyngeal carcinoma. Eur Arch Otorhinolaryngol. 2012; 269:1027–33. https://doi.org/10.1007/s00405-011-1720-x PMID:21706324

29. Ngan RK, Yiu HH, Lau WH, Yau S, Cheung FY, Chan TM, Kwok CH, Chiu CY, Au SK, Foo W, Law CK, Tse KC. Combination gemcitabine and cisplatin chemotherapy for metastatic or recurrent nasopharyngeal carcinoma: report of a phase II study. Ann Oncol. 2002; 13:1252–58. https://doi.org/10.1093/annonc/mdf200 PMID:12181249

30. Zhang Y, Chen L, Hu GQ, Zhang N, Zhu XD, Yang KY, Jin F, Shi M, Chen YP, Hu WH, Cheng ZB, Wang SY, Tian Y, et al. Gemcitabine and Cisplatin Induction Chemotherapy in Nasopharyngeal Carcinoma. N Engl J Med. 2019; 381:1124–35. https://doi.org/10.1056/NEJMoa1905287 PMID:31150573

31. Liu L, Wang T, Yang X, Xu C, Liao Z, Wang X, Su D, Li Y, Zhou H, Qiu X, Chen Y, Huang D, Lian C, Su P. MTNR1B loss promotes chordoma recurrence by abrogating melatonin-mediated β-catenin signaling repression. J Pineal Res. 2019; 67:e12588. https://doi.org/10.1111/jpi.12588 PMID:31140197

32. Zhao H, Wei W, Sun Y, Gao J, Wang Q, Zheng J. Interference with the expression of β-catenin reverses cisplatin resistance in A2780/DDP cells and inhibits the progression of ovarian cancer in mouse model. DNA Cell Biol. 2015; 34:55–62. https://doi.org/10.1089/dna.2014.2626 PMID:25211326

33. Reya T, Clevers H. Wnt signalling in stem cells and cancer. Nature. 2005; 434:843–50. https://doi.org/10.1038/nature03319 PMID:15829953

34. Willert K, Brown JD, Danenberg E, Duncan AW, Weissman IL, Reya T, Yates JR 3rd, Nusse R. Wnt proteins are lipid-modified and can act as stem cell growth factors. Nature. 2003; 423:448–52. https://doi.org/10.1038/nature01611 PMID:12717451

35. Zecca M, Basler K, Struhl G. Direct and long-range action of a wingless morphogen gradient. Cell. 1996; 87:833–44. https://doi.org/10.1016/S0092-8674(00)81991-1 PMID:8945511

36. Blask DE, Brainard GC, Dauchy RT, Hanifin JP, Davidson LK, Krause JA, Sauer LA, Rivera-Bermudez MA, Dubocovich ML, Jasser SA, Lynch DT, Rollag MD, Zalatan F. Melatonin-depleted blood from premenopausal women exposed to light at night stimulates growth of human breast cancer xenografts in nude rats. Cancer Res. 2005; 65:11174–84. https://doi.org/10.1158/0008-5472.CAN-05-1945 PMID:16322268

37. Kim JH, Jeong SJ, Kim B, Yun SM, Choi DY, Kim SH. Melatonin synergistically enhances cisplatin-induced apoptosis via the dephosphorylation of ERK/p90 ribosomal S6 kinase/heat shock protein 27 in SK-OV-3 cells. J Pineal Res. 2012; 52:244–52. https://doi.org/10.1111/j.1600-079X.2011.00935.x PMID:22050627

38. León J, Casado J, Jiménez Ruiz SM, Zurita MS, González-Puga C, Rejón JD, Gila A, Muñoz de Rueda P, Pavón EJ, Reiter RJ, Ruiz-Extremera A, Salmerón J. Melatonin reduces endothelin-1 expression and secretion in colon cancer cells through the inactivation of FoxO-1 and NF-κβ. J Pineal Res. 2014; 56:415–26. https://doi.org/10.1111/jpi.12131 PMID:24628039

39. Fan C, Pan Y, Yang Y, Di S, Jiang S, Ma Z, Li T, Zhang Z, Li W, Li X, Reiter RJ, Yan X. HDAC1 inhibition by melatonin leads to suppression of lung adenocarcinoma cells via induction of oxidative stress and activation of apoptotic pathways. J Pineal Res. 2015; 59:321–33. https://doi.org/10.1111/jpi.12261 PMID:26184924

40. Ho HY, Lin CW, Chien MH, Reiter RJ, Su SC, Hsieh YH, Yang SF. Melatonin suppresses TPA-induced metastasis by downregulating matrix metalloproteinase-9 expression through JNK/SP-1 signaling in nasopharyngeal carcinoma. J Pineal Res. 2016; 61:479–92. https://doi.org/10.1111/jpi.12365 PMID:27600920

41. Zhang J, Li YQ, Guo R, Wang YQ, Zhang PP, Tang XR, Wen X, Hong XH, Lei Y, He QM, Yang XJ, Sun Y, Ma J, Liu N. Hypermethylation of *SHISA3* Promotes Nasopharyngeal Carcinoma Metastasis by Reducing SGSM1 Stability. Cancer Res. 2019; 79:747–59. https://doi.org/10.1158/0008-5472.CAN-18-1754 PMID:30573520

42. Liu N, Tang LL, Sun Y, Cui RX, Wang HY, Huang BJ, He QM, Jiang W, Ma J. MiR-29c suppresses invasion and metastasis by targeting TIAM1 in nasopharyngeal carcinoma. Cancer Lett. 2013; 329:181–88. https://doi.org/10.1016/j.canlet.2012.10.032 PMID:23142282

43. Nakazawa Y, Arai H, Fujita N. The novel metastasis promoter Merm1/Wbscr22 enhances tumor cell survival in the vasculature by suppressing Zac1/p53-dependent apoptosis. Cancer Res. 2011; 71:1146–55. https://doi.org/10.1158/0008-5472.CAN-10-2695 PMID:21148752

44. Cai L, Ye Y, Jiang Q, Chen Y, Lyu X, Li J, Wang S, Liu T, Cai H, Yao K, Li JL, Li X. Epstein-Barr virus-encoded microRNA BART1 induces tumour metastasis by regulating PTEN-dependent pathways in nasopharyngeal carcinoma. Nat Commun. 2015; 6:7353. https://doi.org/10.1038/ncomms8353 PMID:26135619

SUPPLEMENTARY MATERIALS

Supplementary Figures

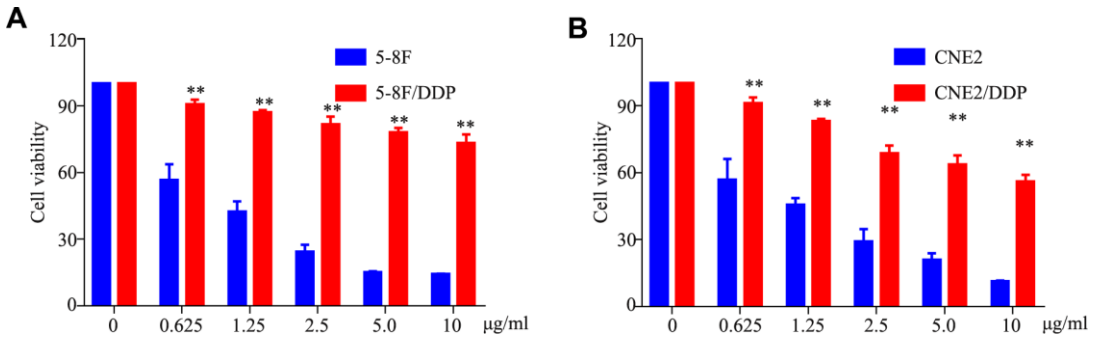

Supplementary Figure 1. Establishment of cisplatin-resistant NPC cells. (**A**, **B**) CCK8 assay was conducted in parental and 5-8F/DDP (**A**) and CNE2/DDP (**B**) cells.

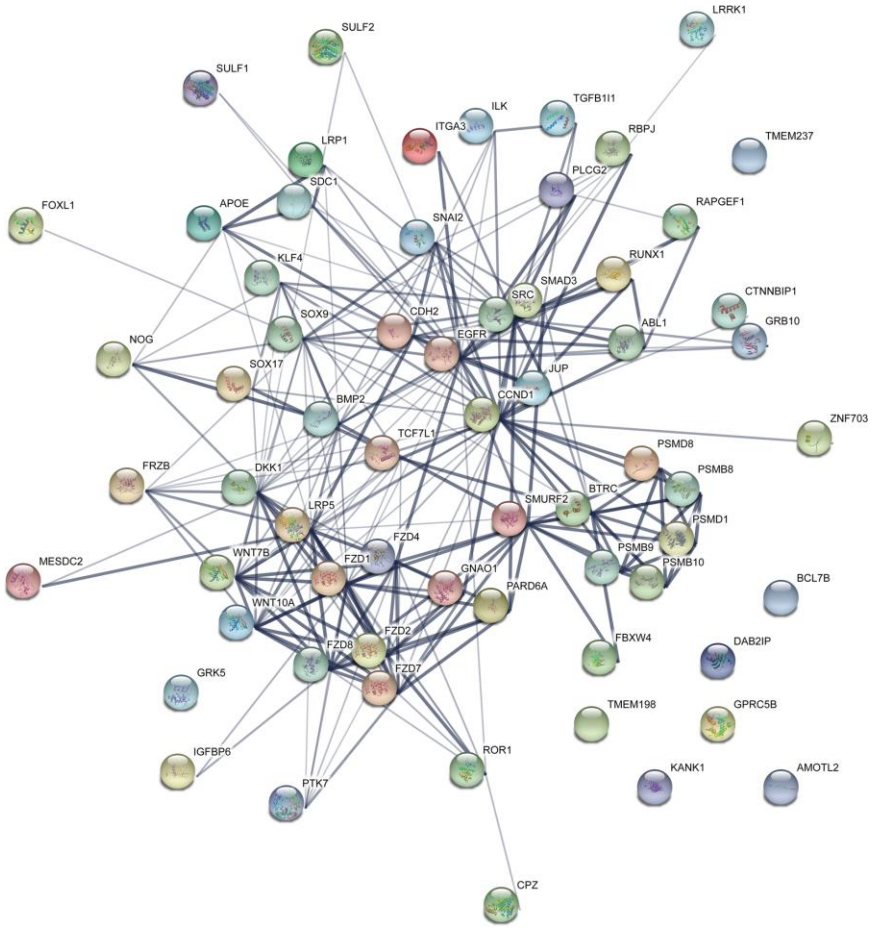

Supplementary Figure 2. Hub genes in the Wnt/β-catenin signaling pathway.

Supplementary Tables

Supplementary Table 1. Primers used in this study.

Gene	Sequence (5' to 3')
CCND2-F	GAGAAGCTGTCTCTGATCCGCA
CCND2-R	CTTCCAGTTGCGATCATCGACG
CD44-F	CCAGAAGGAACAGTGGTTTGGC
CD44-R	ACTGTCCTCTGGGCTTGGTGTT
SOX9-F	AGGAAGCTCGCGGACCAGTAC
SOX9-R	GGTGGTCCTTCTTGTGCTGCAC
AXIN2-F	CAAACTTTCGCCAACCGTGGTTG
AXIN2-R	GGTGCAAAGACATAGCCAGAACC
GAPDH-F	TGATGACATCAAGAAGGTGG
GAPDH-R	TTGTCATACCAGGAAATGAGC

Supplementary Table 2. Antibodies used in this study.

Antibody	Company	Catalog no.	Dilution
Western blot			
β-cantenin	Proteintech	21112-1-AP	1:1000
DDK1	Proteintech	51067-2-AP	1:1000
c-Myc	Proteintech	10828-1-AP	1:2000
CyclinD1	Proteintech	60186-1-Ig	1:5000
GAPDH	Proteintech	51064-2-AP	1:5000
Mouse	CST	7076	1:5000
Rabbit	CST	7074	1:5000
Immunohistochemistry			
Ki67	CST	9949	1:400
β-cantenin	Proteintech	51067-2-AP	1:200
Immunofluorescence			
β-cantenin	Life	51067-2-AP	1:2000
CoraLite594 – conjugated Goat Anti-Rabbit IgG(H+L)	Proteintech	SA00013-4	1:200